

## Article

# Design and Optimization of Free-Form Surfaces for Modular Concrete 3D Printing

Zlata Tošić <sup>\*</sup>, Martin Friedrich Eichenauer <sup>a</sup>, Egor Ivaniuk <sup>b</sup>, Daniel Lordick <sup>a</sup>, Sonja Krasić <sup>c</sup> and Viktor Mechtcherine <sup>b</sup>

- <sup>\*</sup> University of Niš, Faculty of Civil Engineering and Architecture, Aleksandra Medvedova 14, 18000 Niš, Serbia; TU Dresden, Institute of Geometry, Zellescher Weg 12-14, 01069 Dresden, Germany; zлата.tosic@tu-dresden.de/ zлата10@live.com
- <sup>a</sup> TU Dresden, Faculty of Mathematics, Department for Geometry, Zellescher Weg 12-14, 01069 Dresden, Germany
- <sup>b</sup> TU Dresden, Faculty of Civil Engineering, Institute of Construction Materials, Technische Universität Dresden IfB 01062 Dresden, Germany
- <sup>c</sup> University of Niš, Faculty of Civil Engineering and Architecture, Department of Visual Communications, Aleksandra Medvedova 14, 18000 Niš, Serbia

**Abstract:** Shell-like, double curved and thus above-average performance structures, are usually produced monolithically on site. For industrial advancement, however, they must be divided into transportable modules which can be assembled on the construction site (design for assembly). Models are lattice shells made of steel and glass, in which predominantly flat sub-surfaces (modules) are used. Therefore, the main question is: *Which modularizations are suitable for flow production with mineral building materials?* In this paper designed free-form surface is going to be discretized as PQ circular mesh system, suitable modules for 3D concrete printing. Moreover, the multi-criteria optimization is done with Response Surface Methodology (RSM) in order to get optimal final shape. The goal is to start from the arbitrary shape, that can be generated from two curves, with possible two-way division into modules and compare it with the resulted discretized PQ circular mesh system, realized with new algorithm. The comparison can be defined through two main criteria: *geometrical and structural*.

**Keywords:** circular meshes; free-form surfaces; 3D concrete printing; shell structures

## 1. Introduction

Shells as a construction and architectural systems are very efficient structures. Reinforced concrete stays as one of most used materials. Not only because of its possibility to be sculptured into any shape, but also for its strength and ductility. If we look at cost intensity of buildings [1] and the current demographic and economic developments, the demands for cheap, fast and location-independent and flexibly adaptable residential and industrial buildings are becoming increasingly clear [2]. Studies assume a market potential of 520 billion euros in 2020 [3]. To avoid that process, prefabrication of the modules that can be assembled on site is the possible solution. Modularization of the free-form shells can be quite a challenge when over-looking the manufacturing, material, geometry and shape criteria. Discrete differential geometry is promising approach for the free-form shape challenges.

The discretization of concrete shells is prominently used in the Palazetto dello Sport by Pier Luigi Nervi (1957), combining prefabricated parts with in situ concrete [4]. The disassembly was chosen constructively independent of latitudes and meridians. With regard to dry finished parts for shells, Bletzinger [5] and Gehlen [6] have submitted proposals for cutting and production in SPP 1542. However, the important questions about the economic production of the formwork of the freely formed individual parts remain unanswered. The faceting of curved surfaces with flat squares (PQ meshes) according to

manufacturing technology and static aspects is an active research area [7] [8]. The applications are usually steel-glass constructions, in which the squares are stiffened with diagonal ties. Therein lies a creative freedom [9]. The discretization of curved surfaces, in particular the quadrilateral faceting of control surfaces, is the subject of further work by Lordick [10]. At the center of interest are elegant constructions with special curved ruled surfaces that allow exact square faceting due to their geometrical properties.

The work of the BLOCK Research Group (BRG) at ETH Zurich shows how durable constructions, which are essentially pressure-stressed, can be manufactured and joined from relatively small individual parts [11]. Blok [12] also comes up with proposals for the fitting of concrete ceilings by means of special edge shapes. These are geared towards additive manufacturing methods [13]. With regard to curved patches for discretization, in particular hyperbolic paraboloids (HP), the work by Pottmann on ruled surface strips and by Kotnik on the statics of HP patches should be mentioned [14] [15].

## 2. Methods and tools for the production, design and optimization

### 2.1. Technology for the flow production process

As mentioned, the production with 3D printed concrete limits and leads the constraints, therefore defines the geometry and construction limitations when it comes to production modules. There are limitations in the size of the printing area ( $a, b, c, d$  size of edges), specified angles between the edges, for example not sharper than  $45^\circ$  ( $\alpha, \beta, \gamma$  and  $\delta$ ), radius of the corner, thickness of the edge, edge side inclination and different reinforcement placement in the edge and infill (Figure 1 left). One of the biggest problems in the free-form geometry design is the offset option that gives shell the thickness. Depending of the chosen segmentation of these surfaces, not every offset direction will result the flat connection surface between the elements, rather a ruled surface. This is one of the top problems for production as we need to have planar contact surface in between modules. Moreover, the module edge side represents the position of connections, so the geometry of will influence the design and production of connectors as well (Figure 1 right). That limitation brings out the geometry condition called "zero geometry torsion" in the nodes in order to keep the contact surface flat rather than ruled. For this reason, authors turn to methods from discrete differential geometry to enable optimization or construction of efficient geometry shapes. Scalability and adaptability is a must, which means that bigger variation in size and shape will be an issue and will inquire multiple concrete extruders for different size cross sections as well as more printing areas, which is not optimal solution. One of the biggest printing conditions is that the extruder cannot go simultaneously in x-z or y-z direction, which means that modules should be planar. All this influenced a lot the implemented geometry methods that are analysed in the next section.

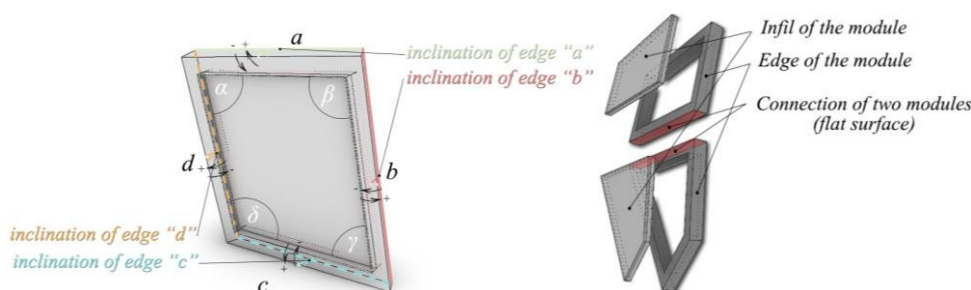


**Figure 1.** Schematic representation of the 3D printing properties of module (left), connection of the two modules with flat edge side (right).

When it comes to construction demands, the forces have to be analysed in the overall structure. Starting from a combination of membrane and bending stress state [16] in the shell-like structure, in the edge zones, which form a lattice structure, predominantly normal forces are decisive. The infill is necessary for the dissipation of the occurring shear stresses, serves to stiffen the module and can experience local bending stresses.

## 2.2. Geometry methods used for the design and optimization

Free-form shape in an arbitrary sense does not have a lot of distinctive properties but discrete differential geometry contributes with one of the largest range of methods for defining their characteristics. The most important geometry property that can reflect the free-form surface are principle curvature directions. Discretization of the free-form surface in the direction of principle curvature lines brings the PQ mesh system [17] [18]. These PQ strips are actually tangent planes of the surface. The authors choose the PQ circular mesh properties to guide them into the process of principle curvature directions, as they represent discrete versions of them [19]. By using their geometrical properties, the process of the free-form shell modulation is generated.

The first one is the circularity of the mesh and its projection on the unit sphere. There are two systems of the discrete normal (Figure 2). The first defines the vector that connects the centre of the unit sphere with the mesh vertices and the second with the centre of the circumcircle. The second system of normals is gained by generating the offset mesh on the constant vertex-vertex distance ( $d - \text{discrete normal} = r - \text{sphere radius}$ ). The first one is used for the measurement of the deviation from geometry torsion free nodes. The second is used as a part of the generating algorithm explained in section 3.3. One of the usage of the second normals is to create the matching PQ system that gives similar shape with potential better preforming results. This could be explored in the future research.



**Figure 2.** Display of the two sets of discrete normals of the circular mesh system on the unit sphere (Tošić et al. 2020).

The principal curvature lines allow for a supporting edge layout with optimal node (placement of vertices in the modular shell) properties. Moreover, the offset mesh property brings a few advantages when it comes to individual elements but also over-all structure.

One of the biggest problems is the geometric torsion in the edges that has large influence on the production of the connections (nodes) with rectangular cross sections. This happens if the symmetry planes of the cross sections of the four elements in a node are not intersecting into a single line (Figure 3 b)). Nevertheless, because of the offset mesh property, that can be avoided, as the vertex-vertex distance (Figure 3 a)) actually defines the node axis and is at the same time normal of the surface in the chosen point. Direction of the offsets can be easily defined through the mapping of the parallel mesh system in the unit sphere (Figure 3 b)).

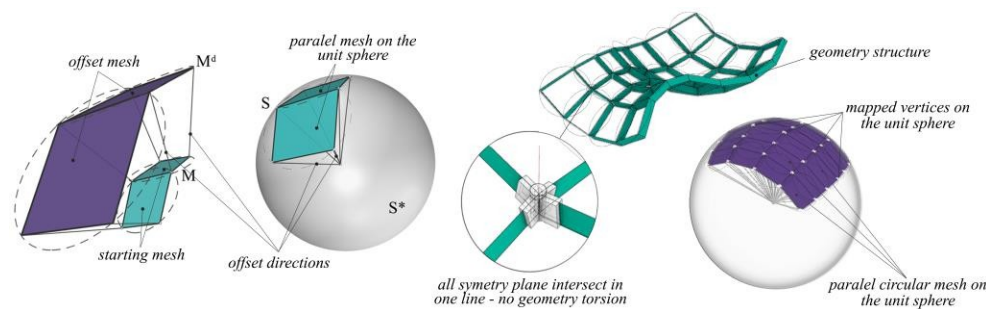


**Figure 3.** a) Mesh offset properties of the circular mesh system within the unit sphere, b) computed for the entire structure [20].

### 3. Workflow

In this section the authors are going to show the workflow of the process of discretization of the free-form shapes that can be generated from two curves. One case study is going to be analysed taking the final chosen solution. The task states: *“Starting from the two curves, generate the free-form PQ circular mesh system with optimal geometry and construction properties for the individual elements and overall construction suitable for 3D concrete printing manufacture.”* The workflow goes as follows:

1. Analysing starting surface for principle curvature and stress directions
2. Choosing the two curves for generation
3. Establishing PQ circular mesh shell
4. Implementing Response Surface Methodology (RSM) for multi-functional optimization and finding the final shape
5. Comparing the starting shell with the final one on the construction and geometry level

#### 3.1. Analysis of the starting free-form shell

Before any intervention on the shell the geometrical and construction features have to be analysed to be able to determine the treatment and potential effectiveness in the usage of the circular PQ mesh system. From the analysis it is important to establish whether are principal directions of curvature and stresses close. Although, the algorithm can make the PQ system for many arbitrary shapes resulting from multiple intersected curves and it is possible to find compromise between the construction and geometry demands in other examples, surfaces with this property are going to have the most potential in this process of PQ circular mesh optimization. This is due to maximum potential of the mentioned edge reinforcement would be used in total for normal forces in the shell. This means that the surfaces geometry complements the construction capacity.

#### 3.2. Determination of the initial curves for generation

The analysis from the previous section is necessary to help us in determination of the initial curves for the process of generation. The idea to start from two curves and try to generate a PQ mesh system is drawn from the research of Tellier [21], where the authors deal only with planar curves as defined edges of the both starting and other discretized curves of the mesh system, which is not the case in this research. Although in showed case study only the starting curves are planar it is possible to use other. The position of the starting curves in the shape depends on the position of principal curvature and stress directions.

If the principal curvature and stress direction are close, the starting choice of curves is determined by the two principal curvature directions in one point on the surface. Depending of the symmetry and shape, it is usually the ones in the middle of the  $u, v$  surface parametrization, or on the symmetry axis, but can be multiple starting points with many intersection curves.



The function of the segmentation algorithm goes *bottom-up* which means that the initial goal is not to approach arbitrary starting shape idea, which is usually done when starting with already defined design that can be in a form of NURBS surface [22]. The goal is to find the right approach within formulated design idea for printable modules with enough freedom in designing shape, with the intention to create better rationalization strategies used in design sequence and their relation to digital fabrication processes [23]. This is achieved by using curves as an input parameter, generating discretized surface, then comparing the resulted PQ mesh system with Rhino/Grasshopper modelling. The control of the final shape goes through the design and relation of the starting curves. Therefore, the system can be used for multiple curves intersection and thus expand the design in more arbitrary surfaces.

### 3.3. Generating the PQ mesh

When it comes to the generation of PQ mesh system the whole procedure has been parametrized in Grasshopper for Rhino with the help of C# coding for circular meshplug in, starting from the input curves to the final results of construction (*forces and deformation*) and geometry properties (*size, shape of the elements and whole shell*). Therefore, it is possible to change the various input curves data and to get the best possible result for geometry and construction.

The algorithm implemented for generating the PQ circular mesh system is based on the geometry characteristics of circular mesh elaborated in the section 2. It starts with two input curves and the number of their division. It recognizes the intersection point and starts to generate the circular quads “one by one” in rows until the end (depending on the number of division on the first and second curve) with the tendency to bring orthogonality between the edges as they are supposed to represent the discretized principle curvature directions. During generation, it also draws the symmetry planes of the two final edges and quad plane (using the second system of normals from section 2.2), where their intersection gives the point which is projected on the starting circle of the quad (Figure 4 right). This should make sure that the geometry torsion is minimal per node (which is measured with the first system of normals if the neighbouring ones are coplanar). The process continues for the next quad as well. Orange gradient represents the flow of the generation starting from first quad (the green one at intersection point) to the last one that is in the end almost transparent on the Figure 4 left.

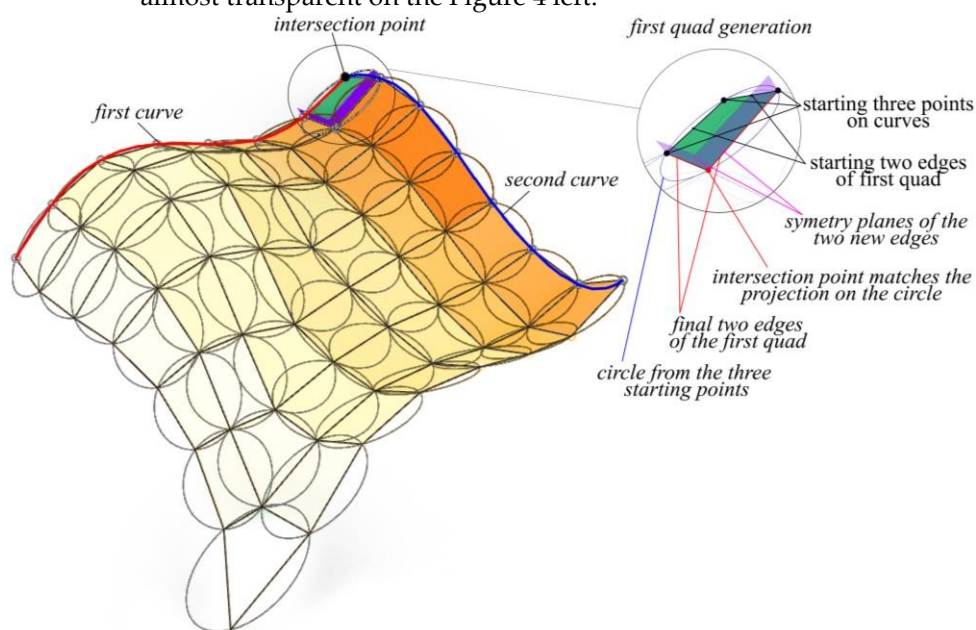


**Figure 4.** Generating PQ circular mesh system from two curves (left), displayed process of every PQ circular quad from three starting points and defined circle (right).

### 3.4. Multi-objective optimization using RSM

As mentioned in the previous section the whole process from the design to the results is parametrized. This brings the possibility to explore how various geometry parameters have impact on the both geometry and construction results and determine the right combination for the final solution. They can be different and start from the design of the shell, types of curves, their position and relation. It implies the usage of methods for extensive multi-objective analysis used in this paper, such as Response Surface Methodology (RSM).

RSM represents a group of mathematical and statistical techniques that are used to define the relationships between the response (result that we are looking for) and independent variables (input parameters that influence result). The most important thing is that RSM can explore, during the process, the influence of independent variables alone and in combination on the result. In addition, the method also generates mathematical model. The term Response Surface Methodology comes from the graphical representation of the mathematical model. The typical equation would look like this:

$$y = f(x_1, x_2, x_3, \dots, x_n) + \varepsilon$$

where the  $f$  is unknown function of response,  $y$  is the response and  $x_1, x_2, x_3, \dots, x_n$  are  $n$  independent variables. The  $\varepsilon$  is the statistical error that represents other sources of variability not implied by  $f$ . This can include effects such as measurement error and it is assumed that its normal distribution is within zero and variance.

In order for the method to be the most successful, it is necessary to determine the optimum settings (ranges of values) and input parameters so that they can result in a maximum (or minimum) response over a certain region of interest,  $R$  [23]. The better is the representation of the input parameters of the model; the bigger chance is to determine the value of the optimum [24]. Vinet and Zhedanov [25] explain this method in detail. In this paper, the Minitab19 is used to run RSM.

### 3.5. Comparing the starting shell with the final one on the geometry and structural level

Lastly, authors compare the final PQ mesh with the initial shape which therefore gets divided in regular  $u, v$  directions. In this way it can be shown how the construction and geometry, but also the manufacturing parameters could be optimized. As a result, recommendations and guidelines for future projects will be given. The next section represents our case study with the implementation of the presented workflow.

## 4. Case study of the shell clover

The initial surface for analysis and optimization is displayed in figure 5. In this case study the surface is generated out of two planar curves with the intersection point on the beginning of both curves. The green curve is concave while the red one is convex, where it can be seen that the whole shell is formed after series of symmetry and rotation transformations. Nevertheless, as mentioned this algorithm does not depend on the number of intersected curves per shape or relation between curves which means that the method doesn't have to be used only for symmetry nor rotational positioning of the curves.

After analysis of the principal curvature and stress directions it is concluded that in this example directions are very close and therefore, the optimization results of this PQ mesh generation have big potential. It must be mentioned that construction analysis was done for support that is continuous on the edge of shell, which is probably not going to be the case in the final construction calculation. The geometry properties are complementing the construction ones, as a result, those directions can be chosen for the PQ generation (red and green curve) and gain minimum change from the initial geometry.

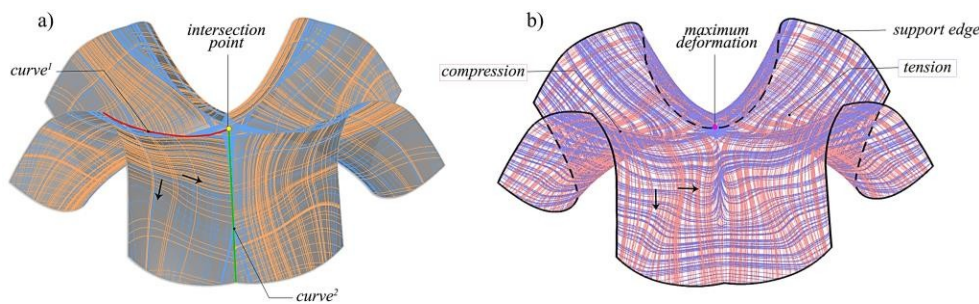


**Figure 5.** Display of the principal curvature directions (left), principle stress directions of the shell(right).

After establishing the starting positions of both curves several input parameters are defined that will be influencing the final outputs. These are: curvature and rotation of both curves, angle between the curves (*the planes where they lay*), number of division (*size and number of the elements*).

The first input parameter that has been considered is angle between the curves' planes followed by the number of curves' division. It influences all the shell properties: *construction, geometry and design*. The idea of the shell design resembles a flower, as a result, the angle between the curves will directly determine the "number of petals" (shell units). Therefore, the possibilities for the angle to fill the 360° circle are: 90° (4 units), 72° (5 units), 60° (6 units) ... to 30° (12 units) (Figure 6).

Based on analysed forces in all four possible solutions, the optimal one (*that has the smallest forces*) was with the angle between the curves' planes 45° (Figure 6a)), which gives eight shell units with the minimum number of division of 10 per curve. This division defines adequate size and shape of the modules for production when it comes to edge angles and size.

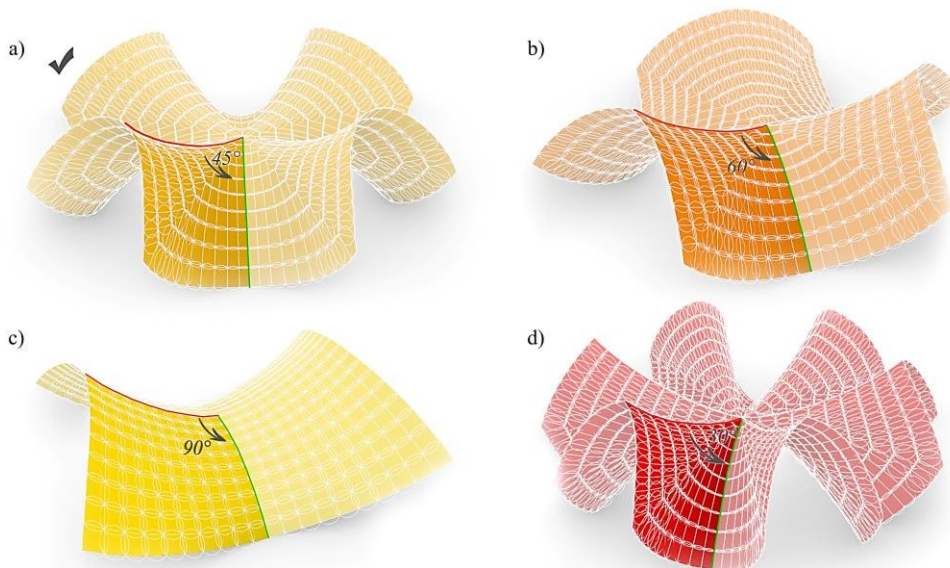


**Figure 6.** Display of the different design results depending on the angle between the curves' planes.

The rest of the parameters are combined together in order to implement the responsive surface analysis (RSM) for the multi-functional optimization and find the optimal shape. In this particular example the input variables are: *curvature of two input curves*, the *rotation angle in their plane around intersection point* and *number of division of curves*. The output variables are two: *normal stress in the edge part of the modules* and *shape operator*. In order to implement the second output the first (angle between curves) input variable had to be determined separately in the first step. Shape operator is defined as distance between

vertices of designed shape and optimal shape for minimizing normal stresses. Several combinations were tested in order to determine the best result.

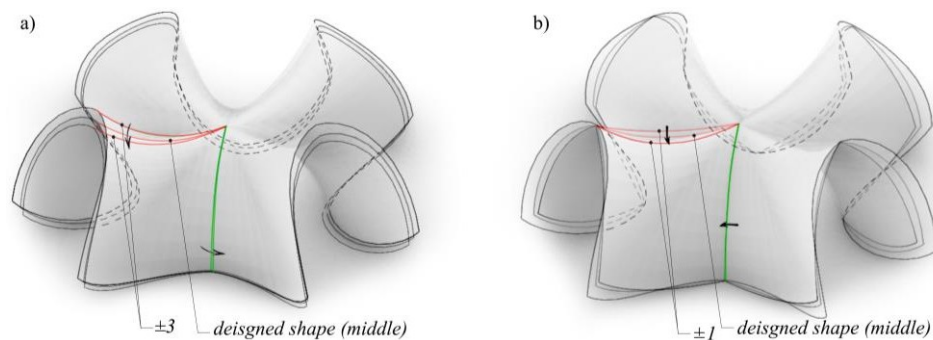


**Figure 7.** Display of the different curves' rotation and curvature in their planes with results of the shell shape.

In order to lower the number of possibilities and tests the range of the input variables was lowered. The angle of the curves could vary  $\pm 3^\circ$  from the starting one (which defined the design shape), the curvature  $\pm 1$  and choice for the number of division was from 10 to 12, as these were the cases of the acceptable sizes of the modules.

The second very important part after calculating necessary combinations for RSM optimization was to determine the relation of the weight of two depending parameters. When there are two output parameters their product is minimized and their weight in the equation can be different. If the parameters are equally important then both have factor  $0.5R_1 * 0.5R_2 = y \Rightarrow \min$ . In this example the weight of the factors is varied in order to determine the best possible result and importance of the variables on the result. These cases are taken into account:  $0.5R_1 * 0.5R_2$ ,  $0.2R_1 * 0.8R_2$ ,  $0.8R_1 * 0.2R_2$ ,  $0R_1 * 1.0R_2$  and  $1.0R_1 * 0R_2$ .

The results of all five combinations of parameters are displayed in the table 1 (for geometry parameters of modules) and as graph (maximal stresses and distortion from designed shape), while the constructions can be seen in the Figure 8. The grey shape overlapped with resulted shells represents the initial design. The first (blue) and fourth (light green) were disregarded since the range between the smallest and biggest elements was very high, so the appropriate scalability condition wasn't satisfied. Moreover, the biggest elements could not fit into the platform of the current 3D concrete printer. The following analysis was the geometry torsion in constructions, according to the cross-section of the modules edges and thickness of the infill. The results show that three of the solutions have no geometry torsion and therefore qualify for further analysis. When the rest of the parameters are compared, the fifth (dark green) is chosen as a final solution, as it has the minimal normal forces and shape distance from the designed model.

**Table 1.** Geometry parameters for production of the modules for all 4 possible solutions.

Geometry parameters for production			
Size of edge modules[m]		Angles between edges	Geometry torsion
Solution 1 (blue)	0.18 – 1.58	45° - 135°	n=128; 2.88°
Solution 2 (orange)	0.29 – 1.24	46° - 134°	/
Solution 3 (yellow)	0.29 – 1.24	46° - 134°	/
Solution 4 (lightgreen)	0.18 – 1.57	45° - 135°	n=128; 2.88°
Solution 5 (darkgreen)	0.34 – 1.47	46° - 134°	/



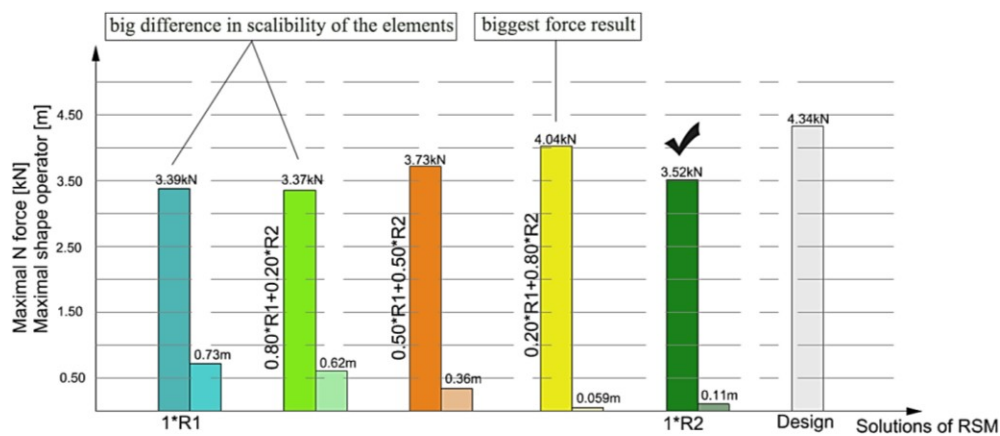


**Figure 8.** Graph showing the maximal normal forces and shape operator for all five solutions (up);Models of all solutions with overlapped designed shape as a reference (grey).

After establishing the final geometry input parameters, the construction was calculated using the Karamba3D Plug-In for Rhino3d. The final modification had to be made for squiring the support and shape of the shell, where some of the elements are cut off at the bottom and on the sides of construction (Figure 9) as well as adding some additional load cases. All knots of the mesh touching the ground are support fixed against translational movement. The elements are separated in the printed edges which get modelled as beams and the infill which get modelled as shell elements. We assume that all elements are connected rigidly. As loads we used common definitions for roof constructions. There are two forces acting on most of the shell element besides self loads, snow and wind forces. For the snow forces we use 0,85kN/m<sup>2</sup> acting in z-direction and for the wind 0,80kN/m<sup>2</sup> acting from one side consider the worst case possible. Because there is a common tolerance in our printing system about 3mm, we also considered forces out of imperfection resulting from a rotation and bending of respectively 1,5 degrees per element. All loads get multiplied with a safety factor of 1,35.

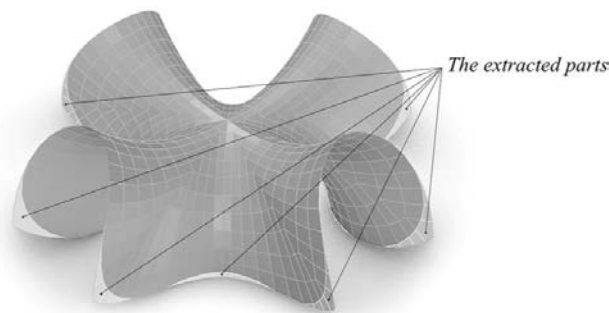


**Figure 9.** The final shape and discretization of the construction (grey) with its extracted parts (lightgrey).

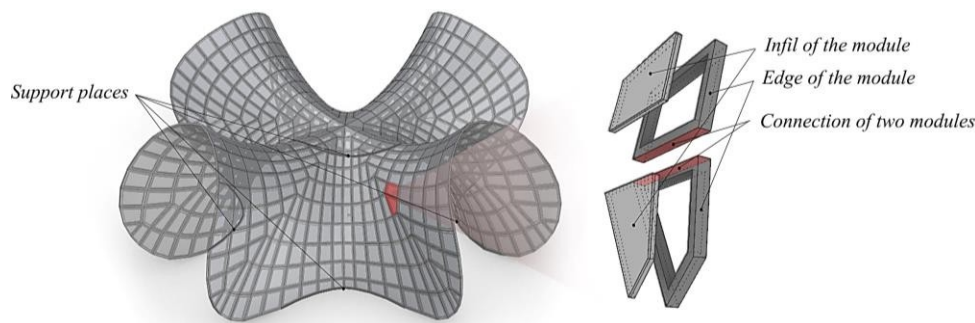


**Figure 10.** Final concrete modular shell construction with support placement (left) details in modules' parts (right).

The geometry and construction properties of the initial shape were also analysed after the chosen position of the curves, but using the standard u, v division. Modules and material properties are treated the same as well as the support placement (Figure10). Depending of the volumetric parametrization of the one shell unit results can vary, but the authors were leaning towards size and shape uniformity of the modules.

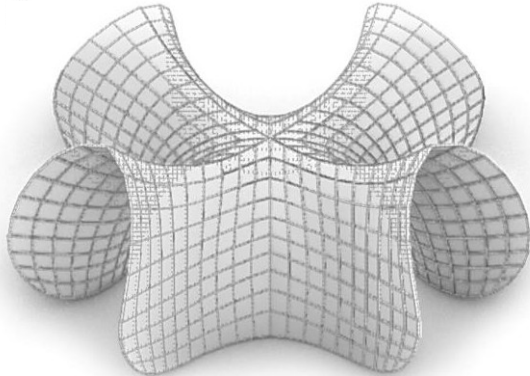


Figure 11. Initial concrete modular shell construction.

5. Results and discussion

In table 2 the results of final and initial shell are compared. When it comes to the construction the optimization can be noticeable in every aspect. The deformation and average utilization of the elements is lowered in the final solution (Figure 12). The axial force (N) in the starting construction is lowered for about 30% with optimized solution for both pressure and tension. Moreover, the final solution enables the less usage of concrete for 4.5% of the mass of starting model.

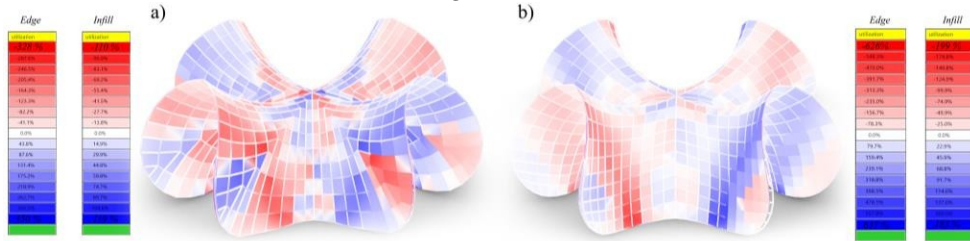


Figure 12. a) Utilization of the edge and infill cross sections in final, b) starting model.

Table 2. Results of the construction and geometry properties of the starting and final construction.

Construction properties				
	Mass [kg]	Deformation	N [kN]	Utilization [%]
Startingmodel	18145	18.32 cm	-16	Infill: aver. 190
			+17	Edge: aver. 630
Finalmodel	17344	9.89 cm	-12	Infill: aver. 115
			+12	Edge: aver. 330

Geometry properties				
Planarity [%]	Geometrytorsion	Number of elements	Edgesize	Angle betweenedges
Startingmodel	7	0° - 21°	0.42 - 0.97	25° - 168°
Finalmodel	0	0°	0.34 - 1.47	46° - 134°

The geometry properties are more suitable for 3D printing when overlooking the fact that final shell has planar modules, whereas in the initial shell modules have maximum

curvature around 7% (Figure 13) (calculated from the average length of mod-ules’ diagonals).

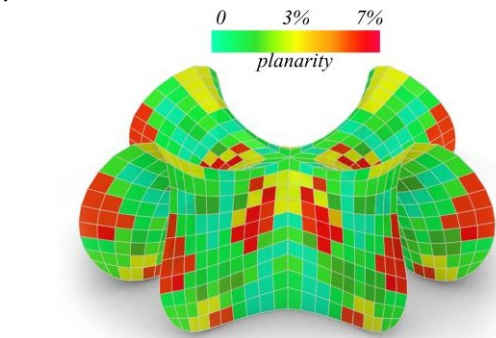


Figure 13. Planarity of the initial shell modules.

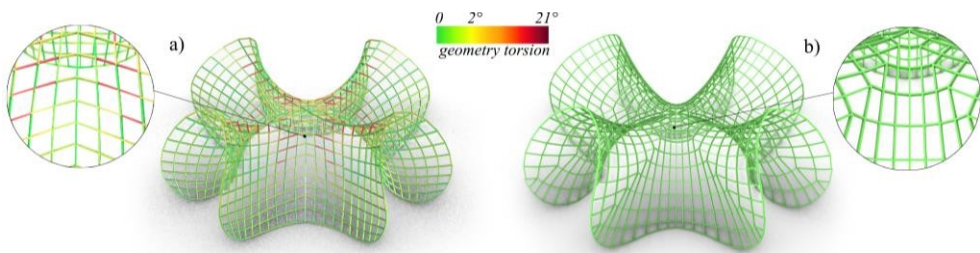


Figure 14. a) Geometry torsion of the starting shell, b) final shell.

The variation of the angle between edges in the initial shell varies from 25° to 168° whereas the final shell’s modules go from 45° to 134°. However, due to the diamondshape of some modules in the final model, the edge size (0.34 m to 1.47 m) varies more than in the starting model (0.42 m to 0.97 m), which can be less suitable for production. When it comes to geometry torsion of the elements in the initial con- struction has elements with curved connection edges up to 21°, while in the final construction has flat edge connection.

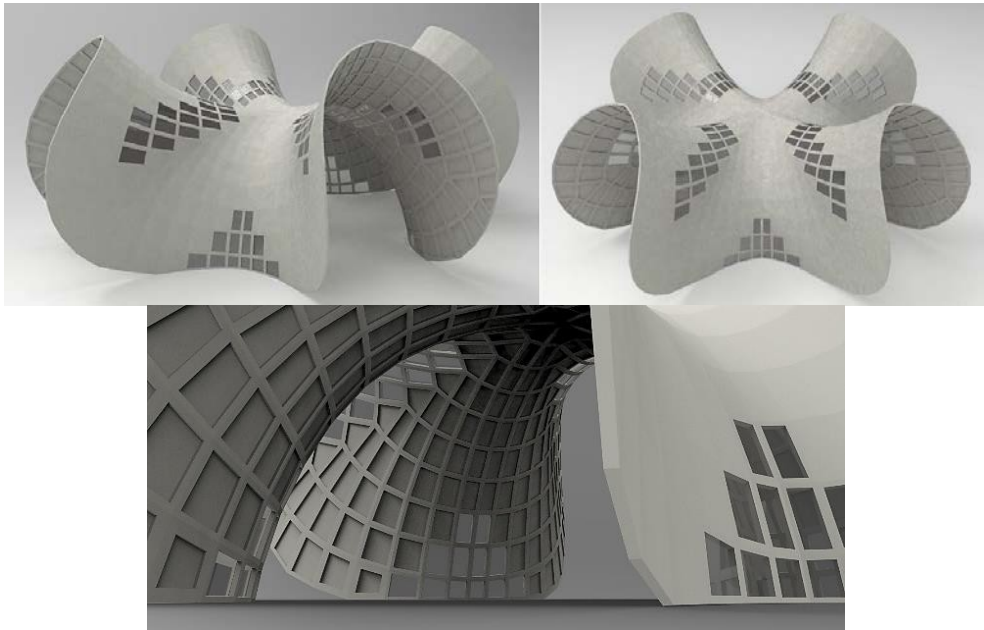


Figure 15. The final design of the modular 3D printed concrete free-form shell.

In the figure 15 the final design can be seen in the form of assembled 3D printed concrete modules. Some of the modules are left without the infill part in the places or lower stresses. As a result, not only the weight of the construction is lowered but also the illumination of the inner space is enabled.

## 6. Conclusion and future research

Circular meshes have big and important place in both design and optimization of the shell constructions. Two curves starting method has benefits as it offers enough initial design limitations, but on the other hand leaves space for establishing very good geometry and construction properties. In this research the authors are using these methods for the purpose of design, optimization and prefabrication of effective modular 3D concrete printing free-form shell structures. As the interdisciplinary nature of the project where the technology and material properties are very important, they have to play out parallel with the geometry and construction conditions that can be very demanding. The biggest advantage, compared to other methods, rise in the needs of the flow production characteristic for the 3D concrete printing such as small variation in the size of the modules, planarity, flat connection surface and normal force edge placement. Moreover, the bottom-up approach that authors use for algorithm is to design and discover more effective shapes that can rise from both planar and space curves.

**Acknowledgements:** The authors would like to acknowledge and express their sincere gratitude to Hani Shahmoradi-Moghadam, who helped in the process of Response Surface Methodology implementation as well as contributing with creative suggestions for its implementation.

**Funding:** This contribution is part of the priority project SPP 2187: Adaptive Modular Construction with Flow Production Methods - Precision High-Speed Construction of the Future in the subproject Formwork-free Flow Production of Adaptive Supporting Structures from Variable Frame Elements - Adaptive Concrete Diamond Construction (ACDC) funded by the German Research Foundation (DFG).

## References

- [1] X. Lee, M. Khamidi, K. S. and C. Heng, "Client-oriented Building Mass Customization (CoBMC)," in *In: IOP Conference Series: Materials Science and Engineering*. Bd. 291, 2017.
- [2] I. Welpé and M. Grundke, "Organisationale Herausforderungen im modularen Hausbau und der Bauwirtschaft," *Der Betriebswirt*, Vol. 58 (2017), Iss. 3; pp. 26-33, 2017.
- [3] M. Grundke and H. Wildemann, "Modularisierung im Hausbau: Konzepte, Marktpotenziale, Wirtschaftlichkeit," *In: Tagungsband des 1. Münchner Kolloquiums Modularisierung im Hausbau*, 2015 München, Germany..
- [4] H. Erwin and S. J., *Kuppeln aller Zeiten, aller Kulturen*, Stuttgart: Deutsche Verlags-Anstalt / DVA, ISBN 13: 9783421030627, 1996.
- [5] M. Breitenberger, W. R. and B. K.U., "Entwurf, Berechnung und Optimierung von gekrümmten Betonfertigbauteilen mit der Isogeometrischen B-Rep Analyse," in *Conference proceedings on building statics building practice 12*, Munich, 2014.



- 
- [6] S. Illguth, G. C. and D. Lowke, "Ultrahigh Strength Fibre-Reinforced Concrete for Thin-Walled Precast Elements," in *Proceedings of the International Association for Shell and Spatial Structures (IASS) Symposium*, Amsterdam, Netherlands, 08/2015.
  - [7] H. A. H. M. K. A. 2. Pottmann, *Architectural Geometry*, Bentley Institute Press, Exton., ISBN:9781934493045 193449304X, 2007.
  - [8] D. Pellis and H. Pottmann, "Aligning principal stress and curvature directions," in *Advances in Architectural Geometry*, Gothenburg, Sweden, September 2018.
  - [9] M. Manahl, M. Stavric and A. Wilsche, "Ornamental discretisation of free-form surfaces: Developing digital tools to integrate design rationalisation with the form finding process," *International journal of architectural computing*, 10 (4), pp. ISSN:1478-0771; pp. 595-612, 2012.
  - [10] D. Lordick, "Intuitive Design and Meshing of Non-Developable Ruled Surfaces," in *Proceedings of the Design Modelling Symposium*, Berlin, Germany, 5-7 October 2009.
  - [11] T. van Mele, A. Mehrotra, T. Mendez Echenagucia, U. Frick, E. Augustynowicz, J. Ochsendorf, M. Dejong and P. Block, "Form finding and structural analysis of a freeform stone vault," in *Proc. of the International Association for Shell and Spatial Structures (IASS) Symposium*, Tokyo, Japan, 2016, September.
  - [12] P. Block, M. Rippmann and T. Van Mele, "Compressive assemblies: Bottom-up performance for a new form of construction," *Architectural Design, Special Issue* 87(4), pp. 104-109, 2017.
  - [13] G. T.-C. Kao, A. Körner, D. Sonntag, L. Nguyen, A. Menges and J. Knippers, "Assembly-aware design of masonry shell structures: a computational approach," in *Proceedings of the IASS Annual Symposium*, Hamburg, Germany, 25th-28th September 2017.
  - [14] S. Flöry and H. Pottmann, "Ruled Surfaces for Rationalization and Design in Architecture," *Life Information. On Responsive Information and Variations in Architecture*, p. pp. 103-109., 2010.
  - [15] T. Cao, J. Schwartz and T. Kotnik, "The global equilibrium of hyperbolic-paraboloid shells based on the method of graphic statics," in *In: Bögle, A., Grohmann, M. (Eds.): Proceedings of the IASS Annual Symposium*, Hamburg, Germany, 25th-28th September, 2017.
  - [16] L. Zhengdao, Q. Geoffrey and X. Xiaolong, "Critical review of the research on the management of prefabricated construction," *Habitat International*, v43 (201407), pp. ISSN:0197-3975, pp. 240-249, 2014.
  - [17] H. Pottmann, S. Brell-Cokcan and J. Wallner, "Discrete surfaces for architectural design," In *Curve and Surface Design*: Avignon, Nashboro Press, pp. 213-234., 2006.
  - [18] H. Pottmann and J. Wallner, "The focal geometry of circular and conical meshes," *Advances in Computational Mathematics*, v29 n3 (200810), pp. ISSN:1019-7168, pp 249-268., 2006.

- 
- [19] H. Pottmann and D. Bentley, *Architectural Geometry*, Exton : Bentley Institute Press, 2012.
- [20] Z. Tošić, S. Krasić, D. Lordick, J. Stanković and N. Kocić, "Discretization and optimization of free form surfaces with circular meshes for adapting to geodesic shell structures," in *MoNGeometrija*, Novi Sad, 2020.
- [21] X. Tellier and O. Baverel, "Surfaces with planar curvature lines: Discretization, generation and application to the rationalization of curved architectural envelopes," *Automation in Construction*, vol. 106, 2019.
- [22] G. Xu, B. Mourrain, A. Galligo and T. Rabczuk, "High-quality construction of analysis suitable trivariate NURBS solids by reparameterization methods," *Computational Mechanics* 54 (5), pp. ISSN:0178-7675, pp. 1303-1313, 2014.
- [23] G. Austern, C. G. I. and Y. J. Grobman, "Rationalization methods in computer aided fabrication: A critical review," *Automation in Construction*, vol. 90, no. <https://doi.org/10.1016/j.autcon.2017.12.027>, pp. 281-293, June 2018.
- [24] A. Khuri and S. Mukhopadhyay, "Response surface methodology," *Wiley Interdiscip. Rev. Comput. Stat.* 2, pp. ISSN:1939-5108, <https://doi.org/10.1002/wics.73>, 128-149, 2010.
- [25] M. Bezerra, R. Santelli, E. Oliveira, L. Villar and L. Escalera, "Response surface methodology (RSM) as a tool for optimization in analytical chemistry," *Talanta* 76, pp. 965-977, 2008.
- [26] L. Vinet and A. Zhedanov, "A "missing" family of classical orthogonal polynomials," *Journal of Physics A: Mathematical and Theoretical*, Volume 44, Number 8, pp. <https://doi.org/10.1088/1751-8113/44/8/085201>, 2011.